11 WCEE

Copyright © 1996 Elsevier Science Ltd
Paper No. 60. (quote when citing this article)
Eleventh World Conference on Earthquake Engineering
ISBN: 0 08 042822 3

IDENTIFICATION OF M,C AND K OF A MULTIPLE DEGREE OF FREEDOM SYSTEM

Yoshihito SAITO and Masaru HOSHIYA

Department of Civil Engineering, Musashi Institute of Technology,
1-28-1 Tamazutsumi, Setagaya-ku, Tokyo, Japan

ABSTRACT

In order to identify the physical parameters including the unknown masses of the structural system, a method using the control force excited by an actuator which is installed on the system is proposed. And a numerical example is demonstrated to show the efficiency of the proposed method where a linear MDOF shear beam with an actuator on the top of floor is taken up as an example structure. As the result, even if all points of the system can not be observed, the proposed method can identify the all physical parameters accurately. Furthermore, it is clarified that the velocity observations are more useful information in the identification than the displacement observations. Then, a field test is carried out for a 23 story building as an actual application.

KEYWORDS

Identification; Kalman filter; Physical parameters; MDOF system

INTRODUCTION

In the case that the dynamic characteristics of structure are identified by using the record data such as earthquake or microtremor , spectrum analyses are used in general. But in this case, it is difficult (Hoshiya *et al.*, 1984a) to identify high frequency modes and damping factors, because it is used to use the smoothed spectrum. The second author of this paper estimates the dynamic characteristics of a four-storied building using the microtremor records, as proposing an approach to estimate the dynamic characteristics of the linear and multidegree of freedom system in tine domain, using the mode characteristics as unknown parameters (Hoshiya *et al.*, 1983, 1984b). There is another approach to estimate indirectly the dynamic characteristics by using the multivariable ARMA model. Toki *et al* (1978) used the least-square method of two orders (PI *et al.*, 1988) , a batch treatment, in order to identify the coefficients of the ARMA model. And the second author of this paper dealed with and identified successively the ARMA coefficients using sequential method with the Karman Filter. The acceleration data such as earthquake motions and microtremors is used as input in such the identification approach for the dynamic characteristics gained from the estimated modal characteristic of the system. It is necessary, however, to know the mass of any arbitrary mass point to estimate the physical parameters such as mass and stiffness. However, as the matter of fact, the mass of a building is not necessarily estimated exactly.

The authors showed an approach to estimate indirectly the physical parameters by using the ARMA model which is excited by vibration control device (Hoshiya *et al.*, 1995). In this case, although the governing equation over the system is easily written, the number of unknown parameters to be identified is more than that of the approach identifying directly the physical parameters.
This paper proposes an approach to identify the physical parameters by using excited force caused by the vibration control device used as input, and investigates the effectiveness of the proposed approach and accuracy of identification in the numerical analysis method.

IDENTIFICATION METHOD OF PHYSICAL PARAMETERS

The extended Kalman filter algorithm is a recursive procedure to estimate the optimal state vector and the corresponding error covariance matrix on the basis of nonlinear continuous state vector equation and nonlinear discrete observation vector equation. The governing equation of the MDOF system which is subject to excitation force at the top is expressed as follows:

$$\mathbf{M}\ddot{\mathbf{X}} + \mathbf{C}\dot{\mathbf{X}} + \mathbf{K}\mathbf{X} = \mathbf{f} \tag{1}$$

where

$\mathbf{M}$: mass matrices
$\mathbf{C}$: viscous damping coefficient matrices
$\mathbf{K}$: stiffness matrices
$\mathbf{X}$: relative displacement vector against the ground
$\mathbf{f}$: excited force vector

It is noted that viscous damping coefficient matrices are assumed to be Rayleigh damping as follows:

$$\mathbf{C} = a_1\mathbf{M} + a_2\mathbf{K} \tag{2}$$

where

$$a_1 = \frac{2\omega_1\omega_2(h_1\omega_2 - h_2\omega_1)}{\omega_2^2 - \omega_1^2} \tag{3}$$

$$a_2 = \frac{2(h_2\omega_2 - h_1\omega_1)}{\omega_2^2 - \omega_1^2} \tag{4}$$

h_i : i-th mode damping coefficient
ω_i : i-th natural circular frequency

If the state vectors are defined as follows,

$$Z_1 = [x_1 \ x_2 \ \cdots \ x_N]^T = [z_1 \ z_2 \ \cdots \ z_N]^T \tag{5}$$

$$Z_2 = [\dot{x}_1 \ \dot{x}_2 \ \cdots \ \dot{x}_N]^T = [z_{N+1} \ z_{N+2} \ \cdots \ z_{2N}]^T \tag{6}$$

$$Z_3 = \left[\frac{k_1}{m_1} \ \frac{k_1}{m_2} \ \frac{k_2}{m_2} \ \cdots \ \frac{k_{N-1}}{m_N} \ \frac{k_N}{m_N}\right]^T = [z_{2N+1} \ z_{2N+2} \ \cdots \ z_{4N-1}]^T \tag{7}$$

$$Z_4 = [a_1 \ a_2]^T = [z_{4N} \ z_{4N+1}]^T \tag{8}$$

$$Z_5 = \left[\frac{1}{m_1}\right] = [z_{4N+2}] \tag{9}$$

Where x = displacement response; $\dot{x}$ = velocity response; m = mass; k = spring constant.

Then, the equation (1) can be rewritten as following state vector equation:

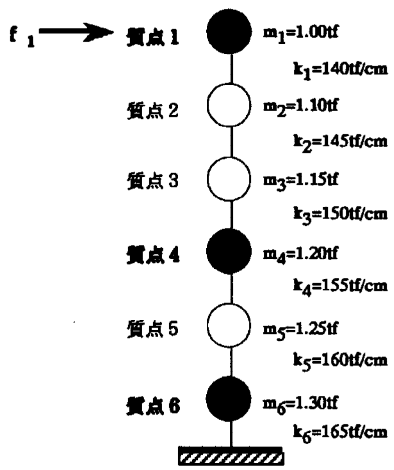

Fig. 1 Analysis model

Table 1. Initial Conditions

state variables	k_1/m_1	k_1/m_2	k_2/m_2	k_2/m_3	k_3/m_3	k_3/m_4	k_4/m_4
Z_0 (Exact Value)	200 (140)	200 (127)	200 (132)	200 (126)	200 (130)	200 (125)	200 (129)
P_0	1000	1000	1000	1000	1000	1000	1000
state variables	k_4/m_5	k_5/m_5	k_5/m_6	k_6/m_6	a_1	a_2	$1/m_1$
Z_0 (Exact Value)	200 (124)	200 (128)	200 (123)	200 (127)	0.06 (0.0425)	0.003 (0.00182)	1.5 (1.0)
P_0	1000	1000	1000	1000	1.0	1.0	1.0

$$\frac{dZ}{dt} = \begin{bmatrix} \dot{Z}_1 \\ \dot{Z}_2 \\ \dot{Z}_3 \\ \dot{Z}_4 \\ \dot{Z}_5 \end{bmatrix} = \begin{bmatrix} Z_2 \\ \left[-M^{-1}C\dot{X} - M^{-1}KX + M^{-1}f\right]_Z \\ O \\ O \\ O \end{bmatrix} \tag{10}$$

Where $[\,]_z$ shows that the contents in $[\,]$ is expressed with the state vectors Z and excited force f. The exact expressions are shown in the APPENDIX(I). And also the state transfer matrices which are adopted on the Kalman filter algorithm are shown in the APPENDIX(II). If all of the displacement or velocity responses or a part of them are observed, the observation vector equation is given as follows:

$$Y = UZ + V \tag{11}$$

Where U is the $[r*(4N+2)]$ matrix which consists of 0 or 1, and V shows the white noise matrix.

Now, the state vector equation [(10)] and the observation vector equation [(11)] are formulated, on which the Kalman filter is applied in order to identify the physical parameters. Furthermore, weighted global iteration method is combined in this paper. It is the remarkable point in this paper that the excited top mass (m_1) is identified, since the excited input force is used instead of the input acceleration as earthquake or microtremor Therefore, all physical parameters are calculated from the identified vector of the equation (7).

NUMERICAL ANALYSES

Analysis Model

The model of the analysis is the multi-degrees of freedom system which is shown in Figure 1. The Rayleigh damping is assumed , which is determined from the first and second modal dampings (both dampings are 2%). The excited input force is the band limited white noise which includes the natural frequency of the system (0.2～0.5HZ) with the sampling interval of 0.02 sec. The initial conditions for this analysis are given in Table 1. Furthermore, all the values of the diagonal components of the weighted coefficient matrix **R** are assumed to be 0.01. And the weighted value of each global iteration is assumed to be 1000. The ratio of the noise against all observation used with each case are 1%, 5% and 10%.

In the case of All Points can be Observed

It is assumed that displacement or velocity responses at each mass point are observed and three cases are considered as follows:

CASE-A1: Both displacement and velocity responses at all mass points can be observed
CASE-A2: Only velocity responses at all mass points can be observed
CASE-A3: Only displacement responses at all mass points can be observed

Shown in Table 2 is the ratio of every physical characteristic value to the corresponding true value, where the former value is calculated from the state vector which is finally identified by global iteration in each case. The mark ^ in this table indicates the estimated value which is identified accordingly. In Fig.2 to Fig.4 illustrated is the transition of the ratio of the mass to the corresponding true value at every mass point determined from the state vector identified by every global iteration in the case of the 10% noise. As observed in the same figures, the values convergent on the true value for the 10% noise by only one iteration in the cases that all the response displacements and velocities are able to be observed, thus giving the identified results that are accurate and stable. In the cases that only the velocities of all the mass points are observable, accurate and stable results are obtained, although the iteration times to coverage increase. On the contrary, the cases in which only the response displacements are observable prove that the values hardly coverage on the true ones. As shown in Table.2, even in these cases, the less become the observed noises, the more accurate are the identified results. The reason that the identified results are more accurate in the adoption of response velocity than of the response displacement as both being the observed values, lies in that the response velocity is involved with all the state values to be identified, but the response displacement is thought to have no relations with the terms concerning damping in the transition matrices shown in APPENDIX(2).

In the case of Partial Points can be Observed

It is assumed that displacement or velocity responses at partial mass points (No1, No4 and No6) are observed and three cases are considered as follows:

CASE-A1: Both displacement and velocity responses at partial mass points can be observed
CASE-A2: Only velocity responses at partial mass points can be observed
CASE-A3: Only displacement responses at partial mass points can be observed

Shown in Table 3 is the ratio of every physical characteristic value to the corresponding true value, where the former value is calculated from the state vector which is finally identified by global iteration in each case. The mark ^ in this table indicates the estimated value which is identified accordingly and the mark - indicates the case of non-convergence. In Fig.5 to Fig.7 illustrated is the transition of the ratio of the mass to the corresponding true value at every mass point determined from the state vector identified by every global iteration in the case of the 5% noise. As observed in the same figures, even if only 3 mass points are observable, the values convergent on the true value in the cases that the only response velocities, or displacements and velocities are able to be observed, thus giving the identified results that are accurate and stable, although the iteration times to coverage increase. On the contrary, as shown in Table.3, the cases in which only the response displacements are observable prove that the values hardly coverage on the true ones, even in the case of 1% noise. Fig.8 and Fig.9 is the transition of the ratio of the mass to the corresponding true value at every mass point in the case of the 10% noise in which only response velocities are observed or both response displacements and velocities are observed. Both Figures show, however the iteration times increase, they are identified with being accurate and stable.

Table 2. Estimated Results (observed all points)

obs. points	observed all points								
responses	disp. and vel.			vel.			disp.		
NOISE	1%	5%	10%	1%	5%	10%	1%	5%	10
$\hat{m}_1/m_1$	1.00	1.00	1.00	1.00	1.00	1.00	1.00	1.00	0.79
$\hat{m}_2/m_2$	1.00	1.00	1.01	1.00	1.00	0.99	1.00	1.00	1.36
$\hat{m}_3/m_3$	1.00	1.00	1.00	1.00	1.00	0.99	1.00	1.00	0.82
$\hat{m}_4/m_4$	1.00	0.99	0.99	1.00	0.99	0.99	1.00	1.01	1.12
$\hat{m}_5/m_5$	1.00	1.00	1.00	1.00	1.00	1.00	1.00	1.00	0.97
$\hat{m}_6/m_6$	1.00	1.00	1.00	1.00	1.00	1.00	1.00	1.00	1.05
$\hat{k}_1/k_1$	1.00	1.00	1.00	1.00	1.00	1.00	1.00	1.01	0.80
$\hat{k}_2/k_2$	1.00	1.00	1.00	1.00	1.00	1.00	1.00	1.00	1.01
$\hat{k}_3/k_3$	1.00	1.00	1.00	1.00	1.00	1.00	1.00	1.00	1.04
$\hat{k}_4/k_4$	1.00	1.00	1.00	1.00	1.00	0.99	1.00	1.00	0.98
$\hat{k}_5/k_5$	1.00	1.00	1.00	1.00	1.00	0.99	1.00	1.01	1.05
$\hat{k}_6/k_6$	1.00	1.00	1.00	1.00	1.00	1.00	1.00	1.00	1.01
$\hat{a}_1/a_1$	1.00	1.01	1.02	1.00	1.01	1.03	1.00	1.00	0.98
$\hat{a}_2/a_2$	1.00	1.00	1.00	1.00	0.99	0.99	1.00	1.00	1.23

Table 3. Estimated Results (observed 3 points)

obs. points	observed 3 points								
responses	disp. and vel.			vel.			disp.		
NOISE	1%	5%	10%	1%	5%	10%	1%	5%	10
$\hat{m}_1/m_1$	0.99	0.99	1.02	1.00	1.01	1.04	0.93	1.26	-
$\hat{m}_2/m_2$	1.00	1.01	0.99	1.00	1.00	0.96	1.52	0.73	-
$\hat{m}_3/m_3$	1.00	0.99	0.97	1.00	0.99	0.97	1.22	1.37	-
$\hat{m}_4/m_4$	1.00	1.00	1.00	1.00	1.00	1.00	0.82	0.99	-
$\hat{m}_5/m_5$	1.00	0.99	0.99	1.00	0.99	0.98	0.36	0.32	-
$\hat{m}_6/m_6$	1.00	1.00	0.98	1.00	1.00	0.99	1.23	1.31	-
$\hat{k}_1/k_1$	1.00	0.99	0.98	1.00	0.99	0.98	0.79	1.16	-
$\hat{k}_2/k_2$	1.00	0.99	1.01	1.00	1.00	1.03	0.66	0.75	-
$\hat{k}_3/k_3$	0.99	1.00	1.00	1.00	1.00	0.99	2.76	1.44	-
$\hat{k}_4/k_4$	1.00	1.00	0.99	1.00	0.99	0.99	1.35	2.34	-
$\hat{k}_5/k_5$	1.00	1.00	1.00	1.00	1.00	1.00	0.92	0.67	-
$\hat{k}_6/k_6$	1.00	1.00	1.00	1.00	1.00	0.99	0.99	0.99	-
$\hat{a}_1/a_1$	0.99	1.02	1.05	1.00	1.01	1.02	0.81	0.56	-
$\hat{a}_2/a_2$	1.02	0.99	0.95	1.00	1.02	1.07	1.50	2.10	-

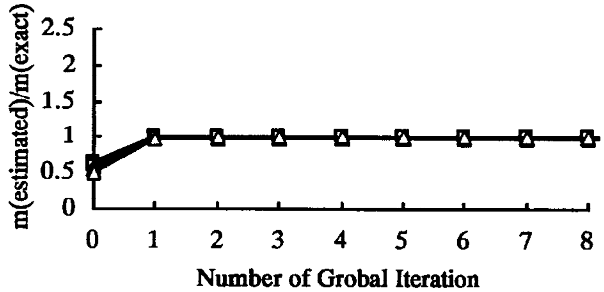

Fig.2 Convergency Process
(observed all points' disp. and vel., 10%noise)

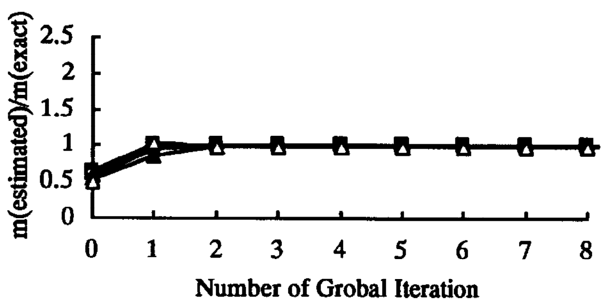

Fig.3 Convergency Process
(observed all points' vel., 10%noise)

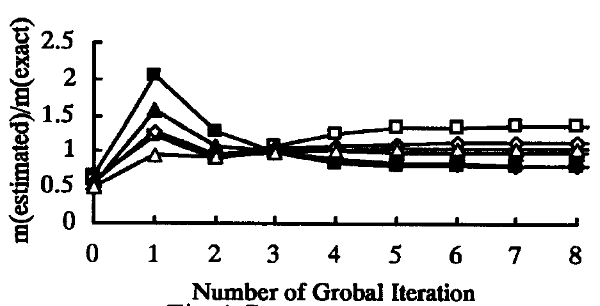

Fig.4 Convergency Process
(observed all points' disp., 10% noise)

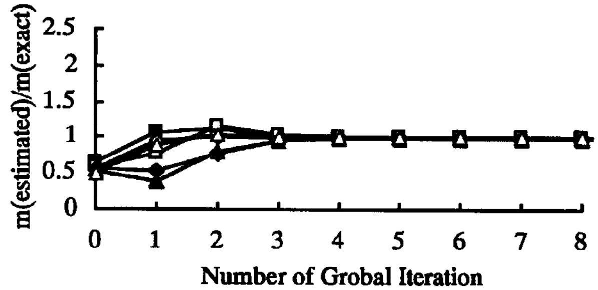

Fig.5 Convergency Process
(observed 3 points' disp. and vel., 5%)

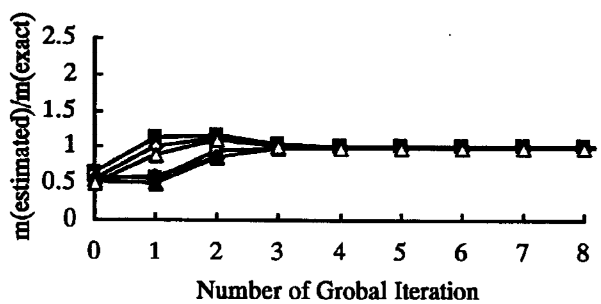

Fig.6 Convergency Process
(observed 3 points' vel., 5%noise)

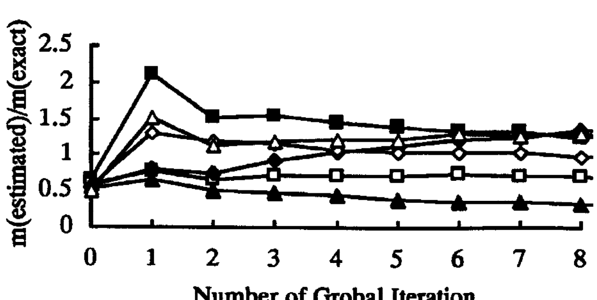

Fig.7 Convergency Process
(observed 3 points' disp., 5% noise)

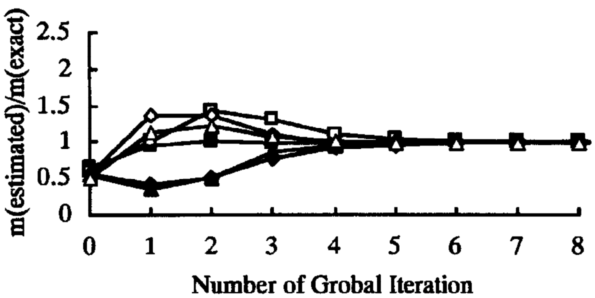

Fig.8 Convergency Process
(observed 3 points' disp. and vel., 10% noise)

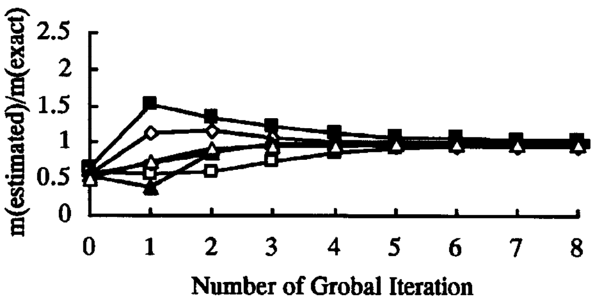

Fig.9 Convergency Process
(observed 3 points' vel., 10% noise)

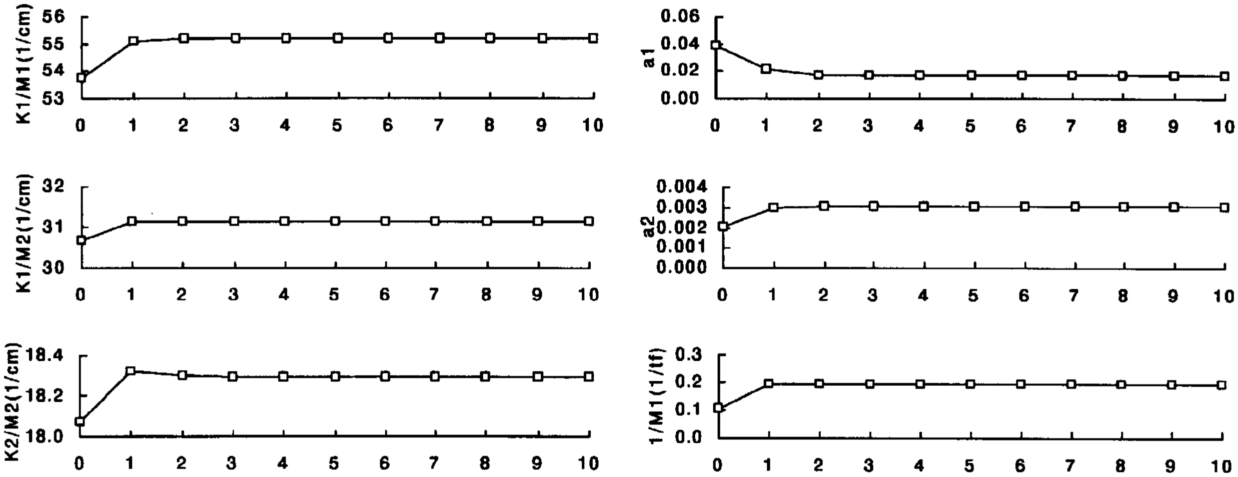

Fig.10 Convergency Process

Table.4 Estimated Physical Parameters

M_1(tfs²/cm)	M_2(tfs²/cm)	K_1(tf/cm)	K_2(tf/cm)	h_1 (%)	h_2 (%)
5	9	282	165	0.77	1.57

Table.5 Comparison between other tests

other vibration test / proposed method	sweep test		free vibration test	
	primary period (sec)	secondary period (sec)	first mode damping (%)	second mode damping (%)
	1.92	0.65	0.93	1.19
	1.92	0.65	0.77	1.57

EXAMPLE AS AN ACTUAL APPLICATION

In order to show the usefulness of the proposed methods, the identification based on the real observed data are carried out for the full-scale and high-rise(23-stories) buildings which is installed with active control device. Since it is the purpose to verify the proposed methods, it is assumed that the system is two degrees of freedom system. The story of the building, where the sensors to sense the responses from the building are to be set up, is decided at the 14th story which is not a node of the mode, as considered from the second degree mode gained from the analysis of the model in the phase of designing, and also the 23rd story where the control device is installed. Each sensor is capable of sensing the response displacement and response velocity at each story. The waveform of control excited force caused by the control device is decided to be the sweep test within the frequency band in the vicinity of the secondary period by considering the result of the free vibration test carried out beforehand. Thus, the responses of the building are thought to be the responsive waveform including the primary and secondary period. We identified each of the state values by means of the proposed approach, using the determined data thereof. Shown in Fig.10 is the convergence of each state value. Each of the state values almost converges on after about three times of the global iteration, thus giving the stable identified results. Physical characteristic values calculated from each state value which was finally identified are as shown in Table.4. Shown in Table.5

are the primary and secondary periods and damping coefficient calculated from the physical characteristic values gained by means of this approach, and the comparison between those values that obtained from the sweep tests as well as the results from free-vibration tests carried out beforehand. The periods of them are coincident with each other and the damping coefficient are also consistent with each other, thus proving adequacy for the results identified by means of this approach.

CONCLUSIONS

A method of directly identifying physical parameters of a linear MDOF system is proposed. Further, a sensitivity analysis has made clear that the stability and convergence are subject to the amount of observation noises, number of observation histories and their locations. Then, a field test is carried out for a 23 story building as an actual application.

As the results, the following points were obtained.

(1) Utilizing the responses of the system excited by an active control device installed, all physical parameters of the system can be identified at any time.

(2) The identification is stable as far as both displacement and velocity histories, or only velocity histories are used and the noise level is less than 10% or so.

(3) If only displacements are observe at a few points, even low noise leads to instability.

(4) It is verified that the proposed method is efficient from an actual application of 23 story building.

This study was performed by the first writer, incorporated with theoretical suggestions by the second writer.

REFERENCES

Hoshiya, M., and Saito, E.(1984a). Identification of Dynamic Properties of a Building by the EK-WGI Method on Microtremor Records. Proc., Japan Soc. of Civ. Engrs., Tokyo, Japan, 350, 263-270(in Japanese).

Hoshiya, M., and Saito, E.(1983). Identification Problem of some Seismic Systems by Extended Kalman filter. Proc., Japan Soc. of Civ. Engrs., Tokyo, Japan, 339, 59-67(in Japanese).

Hoshiya, M., and Saito, E.(1984b). Structural Identification by Extended Kalman filter. J. Engrg. Mech., ASCE, 110(12), 1757-1770.

Hoshiya, M. and Saito, Y.(1995) Prediction Control of SDOF System. J. Engrg. Mech., ASCE, Vol.121 No.10, 1049-1055.

Jazwinski, A.H.(1976). Stochastic Process and Filtering Theory. Academic Pres, New York, N.Y.

Kobori, T.(1990). Technology Development and Forcast of Dynamical Intelligent Building(D.I.B), Intelligent Structures, pp.42-59, Elsevie Applied Science

Kalman, R.E.(1960). A New Approach to Linear Filtering and Prediction Problems. J. Basic Engrg., 82(1), 35-45.

Kalman, R.E., and Bucy, R.S.(1961). New Results in Linear Filtering and Prediction Theory. J. Basic Engrg., 83(1), 95-108.

Maruyama, O., Aizawa J. and Hoshiya, M.(1990). Identification of Dynamic Properties of Existing Structures by Multivariate ARMA Representation. Proc., Japan Soc. of Civ. Engrs., Tokyo, Japan, 416, 439-447(in Japanese).

PI, Y.L. and Mickleborough, N.C.(1988). Time Domain Modal Identification of a linear Vibrating Structure, UNICIV Report R-249, The Univ. of New South Wales, Apr.

Toki, K., Sato, T. and Oiki, Y.(1978). Detection of Dynamic Properties of Structural Systems by the Autoregressive Moving Average Method, Annuals of Disaster Prevention Reseach Institute, Kyoto Univ., 21 B-2, pp.57-68(in Japanese).

APPENDIX (I)

$$\dot{\mathbf{Z}}_2 = \left[-\mathbf{M}^{-1}\mathbf{C}\dot{\mathbf{X}} - \mathbf{M}^{-1}\mathbf{K}\mathbf{X} + \mathbf{M}^{-1}\mathbf{f}\right]_Z$$

$$= \begin{bmatrix}
-(z_{4N} + z_{4N+1}z_{2N+1})z_{N+1} + z_{4N+1}z_{2N+1}z_{N+2} - z_{2N+1}z_1 + z_{2N+1}z_2 + z_{4N+2}f_1 \\
z_{4N+1}z_{2N+2}z_{N+1} - \left[z_{4N} + z_{4N+1}(z_{2N+2} + z_{2N+3})\right]z_{N+2} + z_{4N+1}z_{2N+3}z_{N+3} + z_{2N+2}z_1 - (z_{2N+2} + z_{2N+3})z_2 + z_{2N+3}z_3 \\
z_{4N+1}z_{2N+4}z_{N+2} - \left[z_{4N} + z_{4N+1}(z_{2N+4} + z_{2N+5})\right]z_{N+3} + z_{4N+1}z_{2N+5}z_{N+4} + z_{2N+4}z_2 - (z_{2N+4} + z_{2N+5})z_3 + z_{2N+5}z_4 \\
\vdots \\
z_{4N+1}z_{4N-4}z_{2N-2} - \left[z_{4N} + z_{4N+1}(z_{4N-4} + z_{4N-3})\right]z_{2N-1} + z_{4N+1}z_{4N-3}z_{2N} + z_{4N-4}z_{N-2} - (z_{4N-4} + z_{4N-3})z_{N-1} + z_{4N-3}z_N \\
z_{4N+1}z_{4N-2}z_{2N-1} - \left[z_{4N} + z_{4N+1}(z_{4N-2} + z_{4N-1})\right]z_{2N} + z_{4N-2}z_{N-1} - (z_{4N-2} + z_{4N-1})z_N
\end{bmatrix}$$

APPENDIX (II)

$$\boldsymbol{\Phi} = \begin{bmatrix}
\mathbf{I} & \boldsymbol{\phi}_{12} & \mathbf{O} & \mathbf{O} & \mathbf{O} \\
\boldsymbol{\phi}_{21} & \boldsymbol{\phi}_{22} + \mathbf{I} & \boldsymbol{\phi}_{23} & \boldsymbol{\phi}_{24} & \boldsymbol{\phi}_{25} \\
\mathbf{O} & \mathbf{O} & \mathbf{I} & \mathbf{O} & \mathbf{O} \\
\mathbf{O} & \mathbf{O} & \mathbf{O} & \mathbf{I} & \mathbf{O} \\
\mathbf{O} & \mathbf{O} & \mathbf{O} & \mathbf{O} & \mathbf{I}
\end{bmatrix}$$

where

$$\boldsymbol{\phi}_{12}[N*N] = \begin{bmatrix} \Delta & & \mathbf{O} \\ & \ddots & \\ \mathbf{O} & & \Delta \end{bmatrix}$$

$$\boldsymbol{\phi}_{21}[N*N] = \Delta\begin{bmatrix}
-z_{2N+1} & z_{2N+1} & & & & \mathbf{O} \\
z_{2N+2} & -z_{2N+2} - z_{2N+3} & z_{2N+3} & & & \\
 & z_{2N+4} & -z_{2N+4} - z_{2N+5} & z_{2N+5} & & \\
 & & & \ddots & & \\
 & & & z_{4N-4} & -z_{4N-4} - z_{4N-3} & z_{4N-3} \\
\mathbf{O} & & & & z_{4N-2} & -z_{4N-2} - z_{4N-1}
\end{bmatrix}$$

$$\boldsymbol{\phi}_{22}[N*N] = \Delta\begin{bmatrix}
-z_{4N} - z_{4N+1}z_{2N+1} & z_{4N+1}z_{2N+1} & & & & \mathbf{O} \\
z_{4N+1}z_{2N+2} & -z_{4N} - z_{4N+1}(z_{2N+2} + z_{2N+3}) & z_{4N+1}z_{2N+3} & & & \\
 & z_{4N+1}z_{2N+4} & -z_{4N} - z_{4N+1}(z_{2N+4} + z_{2N+5}) & z_{4N+1}z_{2N+5} & & \\
 & & & \ddots & & \\
 & & & z_{4N+1}z_{4N-4} & -z_{4N} - z_{4N+1}(z_{4N-4} + z_{4N-3}) & z_{4N+1}z_{4N-3} \\
\mathbf{O} & & & & z_{4N+1}z_{4N-2} & -z_{4N} - z_{4N+1}(z_{4N-2} + z_{4N-1})
\end{bmatrix}$$

$\boldsymbol{\phi}_{23}[N*(2N-1)] =$

$$\Delta\begin{bmatrix}
z_{4N+1}(z_{N+2} - z_{N+1}) - z_1 + z_2 & & & & & \mathbf{O} \\
 & z_{4N+1}(z_{N+1} - z_{N+2}) + z_1 - z_2 & z_{4N+1}(z_{N+3} - z_{N+2}) - z_2 + z_3 & & & \\
 & & & z_{4N+1}(z_{N+2} - z_{N+3}) + z_2 - z_3 & z_{4N+1}(z_{N+4} - z_{N+3}) - z_3 + z_4 & \\
 & & & \ddots & & \\
 & & z_{4N+1}(z_{2N-2} - z_{2N-1}) + z_{N-2} - z_{N-1} & z_{4N+1}(z_{2N} - z_{2N-1}) - z_{N-1} + z_N & & \\
\mathbf{O} & & & & z_{4N+1}(z_{2N-1} - z_{2N}) + z_{N-1} - z_N & -z_{4N+1}z_{2N} - z_N
\end{bmatrix}$$

$$\boldsymbol{\phi}_{24}[N*2] = \Delta\begin{bmatrix}
-z_{N+1} & -z_{2N+1}z_{N+1} + z_{2N+1}z_{N+2} \\
-z_{N+2} & z_{2N+2}z_{N+1} - (z_{2N+2} + z_{2N+3})z_{N+2} + z_{2N+3}z_{N+3} \\
-z_{N+3} & z_{2N+4}z_{N+2} - (z_{2N+4} + z_{2N+5})z_{N+3} + z_{2N+5}z_{N+4} \\
\vdots & \vdots \\
-z_{2N-1} & z_{4N-4}z_{2N-2} - (z_{4N-4} + z_{4N-3})z_{2N-1} + z_{4N-3}z_{2N} \\
-z_{2N} & z_{4N-2}z_{2N-1} - (z_{4N-2} + z_{4N-1})z_{2N}
\end{bmatrix}
\qquad
\boldsymbol{\phi}_{25}[N*1] = \Delta\begin{bmatrix} f_1 \\ 0 \\ 0 \\ \vdots \\ 0 \\ 0 \end{bmatrix}$$